Thermodynamic properties of massive dilaton black holes

Takashi Tamaki* and Hiroki Yajima†
Department of Physics, Waseda University, Ohkubo, Shinjuku, Tokyo 169-8555, Japan
(Received 11 April 2001; published 29 August 2001)

We numerically reanalyze static and spherically symmetric black hole solutions in an Einstein-Maxwell-dilaton system with a dilaton potential. We consider two types of potentials: $m_d^2\phi^2$ and $m_d^2S^2(S-1)^2e^{S-1}/4$ where $S:=e^{-2\phi}$, which is proposed based on gluino condensation. We investigate thermodynamic properties in both cases and find that the black hole becomes an extreme solution for a finite horizon radius when a dilaton potential does not vanish. As a result, the Hawking temperature approaches zero in the extreme limit whereas it approaches a finite nonzero value in this limit for the massless dilaton case. This implies that a small amount of the dilaton mass changes the final fate of the black hole.

DOI: 10.1103/PhysRevD.64.084002 PACS number(s): 04.70.−s, 04.40.−b, 95.30.Tg, 97.60.Lf

I. INTRODUCTION

For a long time, the only known stationary and asymptotically flat black hole solutions have been Kerr-Newman solutions which are parametrized by three global charges, a gravitational mass, angular momentum, and an electric (magnetic) charge. Motivated by this fact, the black hole no hair conjecture, which insists that a stationary and asymptotically flat black hole will be decided by these three parameters, was proposed [1]. A black hole solution in the Einstein-Maxwell-dilaton system found by Gibbons and Maeda, and independently by Garfinkle, Horowitz, and Strominger (GM-GHS) was a candidate of a counterexample of the conjecture since it has a global charge related to a dilaton field (a dilaton charge) [2]. Though this black hole does not elude the conjecture, because the dilaton charge is determined by other global charges [3], it has many interesting features. One of the most important is its thermodynamical properties. If we consider the evaporation process of the black hole, its final fate varies depending on the dilaton coupling. For the dilaton coupling $\gamma<1$, its Hawking temperature approaches zero as in the Reissner-Nordström (RN) black hole in the zero horizon limit, while it diverges for the dilaton coupling $\gamma>1$ in the same limit [5]. For the intermediate value $\gamma=1$, it remains a finite nonzero value in this limit. Thus, the thermodynamical properties of the GM-GHS solution are quite distinct from those of the RN black hole. For this reason, Hawking radiation of the GM-GHS solution was investigated in Ref. [6]. It is worth mentioning that those of hairy black holes, which have the Yang-Mills field and the Higgs field, also change qualitatively when the scalar hair such as the Brans-Dicke scalar field is added [7].

However, since a dilaton field has been predicted to have a TeV scale mass and the massless dilaton field is excluded from the experimental aspects [8], we need to investigate black hole solutions with a massive dilaton field in a more realistic case. In this respect, there have been some papers which argued for such black holes and found some interesting properties [9]. For example, these black holes may have three horizons or have wormholes outside the event horizon in the string metric near the extreme solution for the magnetically charged solution. But since including the mass term makes it hard to obtain a solution in a closed analytical form, there remains some room for further investigation. In particular, since thermodynamical properties of these black holes are not exhaustively investigated, we should clarify them. We are interested in how these features are changed by adding a dilaton potential. As for the dilaton potential, since this is not decided from theoretical aspects, we considered two models: one of the simplest models $m_d^2\phi^2$ and a model based on gluino condensation which we will mention below [10].

This paper is organized as follows. In Sec. II we describe our model, basic equations, and boundary conditions. We briefly review the GM-GHS solution in Sec. III. We describe our main results in Sec. IV. For simplicity, we consider the electrically charged solution for the dilaton coupling $\gamma=1$. We denote concluding remarks and future work in Sec. V. Throughout this paper, we use the units $c=\hbar=1$.

II. BASIC EQUATIONS

We take the following type action:

$$S=\int d^4x\sqrt{-g}\left[\frac{R}{2\kappa^2}-\frac{(\nabla\phi)^2}{\kappa^2}-\frac{e^{-2\gamma\phi}}{16\pi g_c^2}F^2-\frac{V(\phi)}{\kappa^2}\right], \tag{1}$$

where $\kappa:=\sqrt{8\pi G}$, ϕ is a dilaton field, and $V(\phi)$ is a dilaton potential. g_c and γ are the coupling constant of the Maxwell field and that of the dilaton field, respectively. The Einstein equations, the dilaton equation, and the Maxwell equation are written as follows:

$$G_{\mu\nu}=2\nabla_\mu\phi\nabla_\nu\phi+\frac{\kappa^2}{4\pi g_c^2}e^{-2\gamma\phi}F_\mu^\lambda F_{\nu\lambda}-g_{\mu\nu}\left[(\nabla\phi)^2-\frac{\kappa^2}{16\pi g_c^2}e^{-2\gamma\phi}F^{\alpha\beta}F_{\alpha\beta}-V\right], \tag{2}$$

*Electronic address: tamaki@gravity.phys.waseda.ac.jp
†Electronic address: yajima@gravity.phys.waseda.ac.jp

$$\Box\phi+\frac{\gamma\kappa^2}{16\pi g_c^2}e^{-2\gamma\phi}F^{\mu\nu}F_{\mu\nu}-\frac{1}{2}\frac{dV(\phi)}{d\phi}=0, \tag{3}$$

$$\nabla_\mu F^{\mu\nu}-2\gamma(\nabla_\mu\phi)F^{\mu\nu}=0. \tag{4}$$

We consider the static and spherically symmetric metric as

$$ds^2=-f(r)e^{-2\delta(r)}dt^2+f(r)^{-1}dr^2+r^2d\Omega^2, \tag{5}$$

where $f(r):=1-2Gm(r)/r$. We choose a gauge potential A_μ as

$$A_\mu=(A(r),0,0,Q_m\cos\theta), \tag{6}$$

where Q_m is a magnetic charge. An electric charge Q_e is defined as $rA(r)\to Q_e$ as $r\to\infty$. We do not consider a dyonic black hole which has both an electric and a magnetic charge below. So we can get basic equations as

$$Gm'=\frac{r^2}{2}(f\phi'^2+B+V), \tag{7}$$

$$\delta'=-r\phi'^2, \tag{8}$$

$$A'=\frac{Q_e}{r^2}e^{-\delta}e^{2\gamma\phi}, \tag{9}$$

$$\phi''+\frac{2\phi'}{r}+\frac{1}{f}\left[\phi'\left\{\frac{2Gm}{r^2}-r(B+V)\right\}+\frac{\kappa^2\gamma}{8\pi g_c^2}\left(-\frac{Q_e^2}{r^4}e^{2\gamma\phi}+\frac{Q_m^2}{r^4}e^{-2\gamma\phi}\right)-\frac{1}{2}\frac{dV}{d\phi}\right]=0, \tag{10}$$

where $':=d/dr$ and we use the abbreviation as

$$B:=\frac{\kappa^2}{8\pi g_c^2}\left(\frac{Q_e^2}{r^4}e^{2\gamma\phi}+\frac{Q_m^2}{r^4}e^{-2\gamma\phi}\right). \tag{11}$$

We consider two dilaton potentials. One is the simplest model, $V_1=m_d^2\phi^2$ where m_d is the dilaton mass and the other is $V_2=m_d^2S^2(S-1)^2e^{S-1}/4$ where $S:=e^{-2\phi}$, which was proposed based on gluino condensation [10]. Though there are a few free parameters in the original paper, we use a simplified model where a potential minimum is achieved by $\phi=0$ (or $\phi=\infty$). In this case, the boundary conditions at spatial infinity to satisfy the asymptotic flatness are

$$m(\infty)=:M=\text{const.},\quad \delta(\infty)=0,\quad \phi(\infty)=0. \tag{12}$$

We also assume the existence of a regular event horizon at $r=r_h$. So we have

$$m_h=\frac{r_h}{2},\quad \delta_h<\infty,\quad \phi_h<\infty, \tag{13}$$

$$\phi_h'=\frac{r(dV_h/d\phi-2\gamma B_h)}{2\{1-r_h^2(B_h+V_h)\}}. \tag{14}$$

The variables with subscript h mean that they are evaluated at the horizon. We will obtain the black hole solution numerically by determining ϕ_h iteratively to satisfy these conditions. For our numerical calculation, we use the Bulirsch-Stoer method based on Ref. [11]. This is the double precision FORTRAN program. To estimate the error, we describe its detail below.

III. THE GM-GHS SOLUTION

First, we briefly explain the GM-GHS solution, i.e., the massless dilaton black hole, to compare with the massive dilaton black hole. To describe the exact solution, it is convenient to use the following spherically symmetric ansatz:

$$ds^2=-\lambda^2dt^2+\frac{1}{\lambda^2}dr^2+R^2d\Omega^2, \tag{15}$$

where λ and R are functions of r only.

We consider the electrically charged case. Since this system has an electric-magnetic duality $F\to e^{-2\phi}\tilde{F}$, $\phi\to-\phi$, we can easily obtain the results for the magnetically charged case. In the above ansatz, we obtain

$$e^{2\phi}=\left(1-\frac{r_-}{r}\right)^{2\gamma/(1+\gamma^2)}, \tag{16}$$

$$\lambda^2=\left(1-\frac{r_+}{r}\right)\left(1-\frac{r_-}{r}\right)^{(1-\gamma^2)/(1+\gamma^2)}, \tag{17}$$

$$R=r\left(1-\frac{r_-}{r}\right)^{\gamma^2/(1+\gamma^2)}, \tag{18}$$

where we chose the asymptotic value of the dilaton field 0. r_+ and r_- are the event horizon and the inner horizon, respectively. They are related to the gravitational mass M and charge Q_e by

$$M=\frac{r_+}{2}+\left(\frac{1-\gamma^2}{1+\gamma^2}\right)\frac{r_-}{2}, \tag{19}$$

$$Q_e=\left(\frac{r_+r_-}{1+\gamma^2}\right)^{1/2}. \tag{20}$$

The solution above has many interesting features, one of which is that the inner horizon is singular and this singularity is spacelike for any nonzero value of γ. The second feature is its thermodynamical properties. The temperature T is written as

$$T=\frac{1}{4\pi r_+}\left(1-\frac{r_-}{r_+}\right)^{(1-\gamma^2)/(1+\gamma^2)}, \tag{21}$$

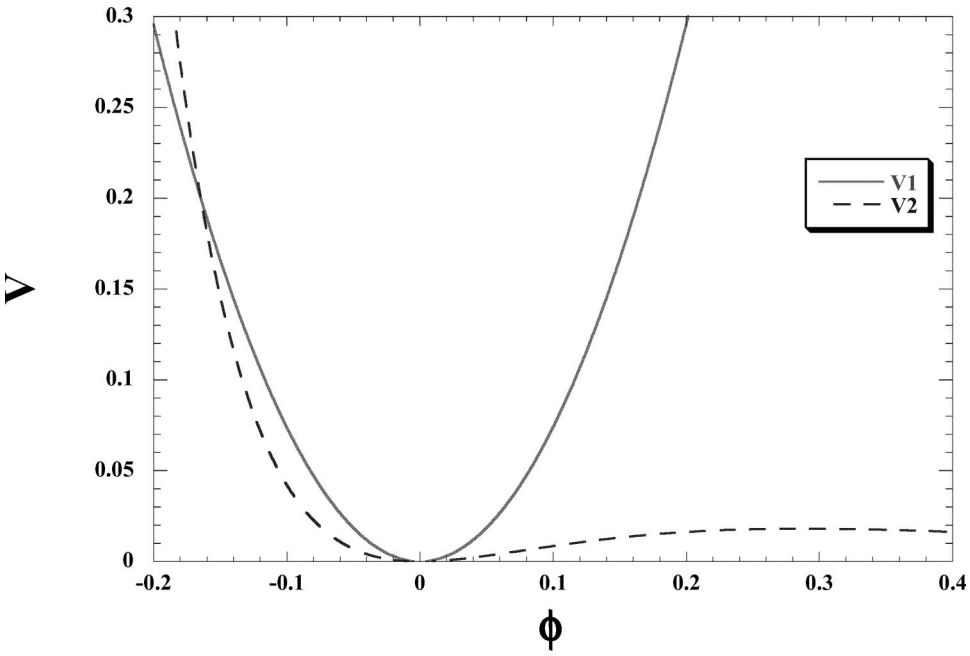

FIG. 1. Shapes of the dilaton potentials for $V_1=m_d^2\phi^2$ and $V_2=m_d^2S^2(S-1)^2e^{S-1}/4$ where $S=e^{-2\phi}$ with $m_d=e/2Q_e$. V_2 approaches V_1 near the bottom of the potential $\phi=0$.

which means that it vanishes in the extreme limit for $\gamma<1$, whereas it has a finite value $1/(8\pi M)$ for $\gamma=1$ and diverges for $\gamma>1$ in the same limit. Thus, these differences are caused by the dilaton field and considering this for the massive dilaton black hole is one of our basic motivations.

IV. PROPERTIES OF MASSIVE DILATON BLACK HOLE

Here, we consider the two dilaton potentials described above and show the shapes of these potentials in Fig. 1 for $m_d=e/2Q_e$ [below, we use e as exp(1) *not* as an electric charge]. As we can see in this diagram, they have a common minimum point at $\phi=0$ around which V_2 is approximated as $m_d^2\phi^2$. When V is an even function, since this system also has an electric-magnetic duality, we can also obtain the results for the magnetically charged case from the electrically charged case [9]. But since V_2 is not an even function, this system does not have such a symmetry in this case.

We summarize the results in previous papers which do not depend on the dilaton potential V whenever V is convex [9]. For the potential V_2, though this condition is not satisfied, ϕ is required to have its value around the convex part to satisfy the asymptotic flatness. So the following results apply in both potentials. (i) The dilaton is monotonically increasing (decreasing) outside the horizon for the electrically (magnetically) charged solution. (ii) For $Q_em_d\lesssim 1$ (or $Q_mm_d\lesssim 1$ for the magnetically charged case), there can be only one horizon. Other properties such as the number of horizons for $Q_em_d\gtrsim 1$ or thermodynamical properties may depend on the shapes of the potential. Thus, we treat each case separately. For simplicity, we choose $\gamma=1$, which is expected from string theoretical aspects.

A. With $V_1=m_d^2\phi^2$

We show field distributions of the massive dilaton black hole [(a) r-ϕ, (b) r-δ, (c) r-m] with horizon radius $r_h=1.1\sqrt{G}$ and the dilaton mass $m_d=e/Q_e$, $e/2Q_e$ by solid lines in Fig. 2. (Below, we normalize as $\sqrt{G}Q_e/g_c\to Q_e$.) For comparison, we also show those of the GM-GHS solution with the dilaton coupling $\gamma=1$ by dotted lines. In Fig. 2(a) we can see the intrinsic difference of the dilaton field with a mass term in comparison to the massless dilaton field. For the GM-GHS solution, the dilaton field behaves as $e^{2\phi}\sim 1+2\Sigma/r$ in the asymptotic region, where Σ is a dilaton charge. It is expressed as

$$\Sigma=-\frac{Q_e^2}{2M}. \tag{22}$$

So it is known as a secondary charge since it is completely determined by the gravitational mass and the electric charge. On the contrary, for the massive dilaton black hole, since Eq. (10) can be approximated as

$$B=\frac{1}{2}\frac{dV}{d\phi}, \tag{23}$$

in the asymptotic region, the dilaton field behaves as $\phi\sim -Q_e^2/m_d^2r^4$ [9]. We also plotted the approximate solution $\phi=-Q_e^2/m_d^2r^4$ by dashed lines to show its consistency. We can find that this approximation is considerably accurate for the distance more than several times the event horizon. From this behavior we can naturally guess that the dilaton field has a scale comparable to its Compton wavelength $\sim 1/m_d$. Thus, the dilaton charge is lost because of the dilaton potential. Moreover, the solution is expected to approach the RN solution since the influence of the dilaton field becomes negligible for large m_d. This behavior may influence other structures. Actually, a wormhole structure outside the event horizon in the string metric, which is absent for the GM-GHS solution, near the extreme black hole of the magnetically charged case is reported in Ref. [9]. Here, we concen-

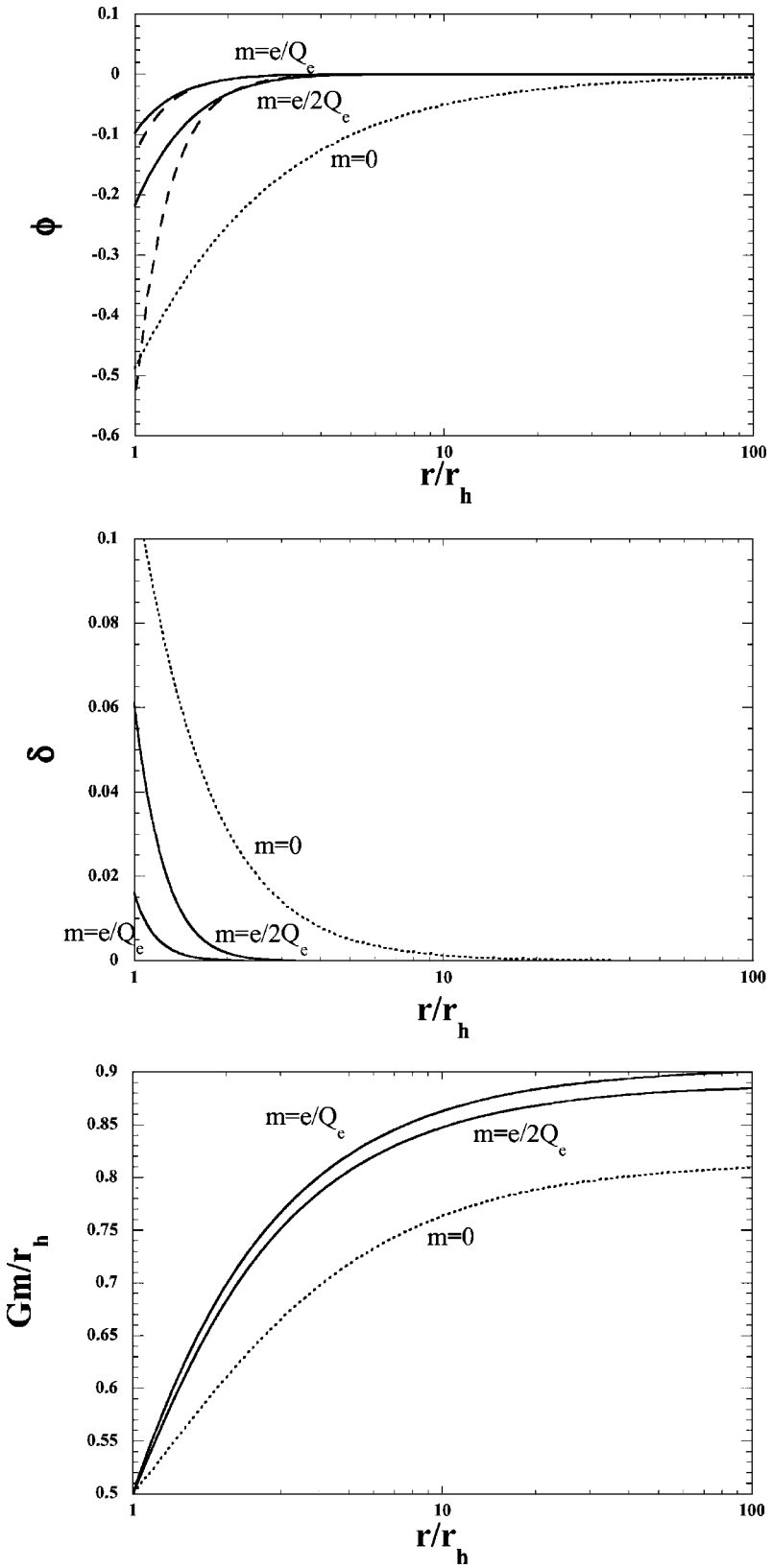

FIG. 2. Field distributions of the massive dilaton black hole with the potential V_1 [(a) r-ϕ (b) r-δ, (c) r-m] with horizon radius $r_h = 1.1\sqrt{G}$ and the dilaton mass $m = e/Q_e$, $e/2Q_e$ by solid lines. For comparison, we also show the GM-GHS solution and the approximate solution by dotted lines and dashed lines, respectively.

trate on its dependence on gravitational mass. Basically, the gravitational mass outside the horizon is made up of three factors: (i) the kinetic term of the dilaton ϕ'^2, (ii) the electromagnetic term B and (iii) the dilaton potential V. To investigate it, it is appropriate to see the lapse function δ which consists of the kinetic term of the dilaton field. As we can see in Fig. 2(b), the massless dilaton field has the largest contribution to this term. On the other hand, the gravitational mass takes the greatest value for the most massive dilaton case as we can see in Fig. 2(c). Since the difference of the electro-

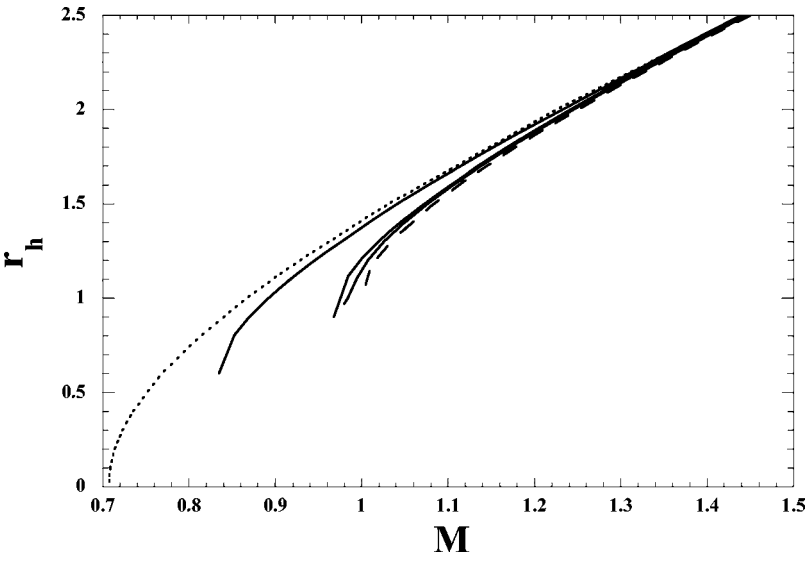

FIG. 3. The relation between the horizon radius r_h and the gravitational mass M of the black holes. We choose the mass of the dilaton as $m=e/10Q_e$, $e/2Q_e$, and e/Q_e and show the massive dilaton black holes, the GM-GHS solution, and the RN solution by solid lines, by a dotted line, and by a dashed line, respectively.

magnetic term B caused by the mass of the dilaton is fairly small, we can naturally conclude that the contribution from the potential term for the gravitational mass is most crucial among the three terms.

Next, we turn our attention to sequences of solutions, when we consider solutions of various horizon radii. Since the dilaton field has a scale comparable to its Compton wavelength, we can expect a qualitative difference depending on the scale of the horizon radius. We consider the condition for the existence of a degenerate horizon along the similar line in Ref. [9]. If the horizon becomes degenerate at $r_h=r_d$, the following condition should be satisfied from Eqs. (7) and (10):

$$1=\frac{Q_e^2e^{2\phi_d}}{r_d^2}+m_d^2\phi_d^2r_d^2, \tag{24}$$

$$0=\frac{Q_e^2e^{2\phi_d}}{r_d^2}+m_d^2\phi_dr_d^2. \tag{25}$$

Note that the finiteness of ϕ_d and ϕ_d' at $r_h=r_d$ are also assumed implicitly. From them, we obtain

$$\frac{1}{\phi_d(\phi_d-1)m_d^2}=r_d^2, \tag{26}$$

$$-\frac{e^{-2\phi_d}}{\phi_d(\phi_d-1)^2}=Q_e^2m_d^2. \tag{27}$$

As we mentioned above, since the dilaton is monotonically increasing outside the horizon for the electrically charged case, ϕ_d is restricted as $\phi_d<0$. In this case, the left-hand side of Eq. (27) reaches its minimum value $e^2/4$ at $\phi_d=-1$. Thus, the solution for $Q_e^2m_d^2<e^2/4$ does not have an extreme limit, *if ϕ_d and ϕ_d' have finite values.* In determining whether this is true or not, we should solve the solutions numerically. We show the relation between the horizon radius r_h and the gravitational mass M of the massive dilaton black hole by solid lines in Fig. 3. We choose the mass of the dilaton field as $m_d=e/10Q_e$, $e/2Q_e$ and e/Q_e. We also write the GM-GHS and the RN solutions by a dotted line and by a dashed line, respectively. Since the event horizon of the RN solution is expressed as

$$r_h=GM+\sqrt{(GM)^2-Q_e^2}, \tag{28}$$

the solution becomes extreme for $Q_e=GM$ where $dr_h/dM=\infty$. For the GM-GHS solution, the extreme solution is realized in the $r_h\to0$ limit where $dr_h/dM=\infty$. $dr_h/dM=\infty$ in the extreme limit is a direct consequence of the first law of black hole thermodynamics. If we fix the electric charge, we can express it as

$$\frac{dr_h}{dM}=\frac{1}{2\pi r_hT}. \tag{29}$$

For the RN and the GM-GHS solutions, T approaches zero (for finite r_h) and r_h approaches zero (for finite T), respectively.

Contrary to the GM-GHS solution, our calculation shows that there is an extreme solution for the finite horizon radius for the massive dilaton black hole even if the mass of the dilaton is very small. We infer that the horizon radius of the extreme solution converges to zero in the $m_d\to0$ limit. Related to this topic, we should mention the validity of our numerical calculation. To guarantee the asymptotically flatness, we judge it from the behavior of the mass function $m(r)$. Because of the potential term in Eq. (7), we need to fine tune the value of ϕ_h. This becomes difficult if the solution approaches the extreme solution since ϕ_h diverges as in the GM-GHS solution. We stop the calculation if we fail to estimate the asymptotic value of $m(r)$ below a few percent. For a reference, we exhibit examples of the asymptotic values of $m(r)$ for $r_h=1.1\sqrt{G}$ with $m_d=e/10Q_e$, $e/2Q_e$, and e/Q_e in Table I.

Existence of the extreme solution suggests the inner horizon. As was shown in previous papers there is no inner horizon for large black holes, while there appears an inner ho-

TABLE I. Examples of the asymptotic values of $m(r)$ for $r_h = 1.1\sqrt{G}$ with $m_d = e/10Q_e$, $e/2Q_e$, and e/Q_e.

m_d	$e/10Q_e$	$e/2Q_e$	e/Q_e
$M\sqrt{G}$	0.9117	0.9858	0.9941

rizon for small black holes. Since we need fine tuning of the dilaton field ϕ to satisfy the regularity at the inner horizon, curvature singularity appears there in general and is spacelike as in the GM-GHS solution. This kind of structure, i.e., where there is an inner horizon for small mass black holes though there is not one for large mass black holes, is also found in charged black holes with Born-Infeld–type nonlinear electrodynamics [12]. It is also worth mentioning that the inner horizon disappears in the Born-Infeld type black hole if we include the dilaton field [13]. Even if there is no inner horizon, the solution does not approach the GM-GHS solution toward the singularity, though the contribution from the potential term diminishes toward the singularity in the basic equations. This apparent discrepancy can be solved using the singularity analysis performed in Ref. [9], i.e., the basic equations with $m_d = 0$ permit a local solution at $r = 0$ of five free parameters. The GM-GHS solution corresponds to one of the special solutions and the massive dilaton black hole approaches one of the other ones toward the singularity. Though the possibility of having three horizons for a massive dilaton black hole is pointed out in previous papers [9], this does not appear. This is because it needs fine tuning both for the mass of the dilaton field (it should satisfy $m_d^2 Q_e^2 = e^2/4$.) and the value of the dilaton field at the horizon (ϕ_h should be -1). Since the dilaton field tends to diverge at the horizon in the extreme limit, this condition is not satisfied.

The most striking feature caused by the dilaton potential is seen in the relation between the gravitational mass M and the inverse Hawking temperature $1/T$ in Fig. 4 for the same solutions as in Fig. 3. For the GM-GHS solution, the temperature remains a finite nonzero value. This is because the extreme limit coincides with the zero horizon limit, which can be easily seen if we express the temperature by the ansatz (5) as

$$T = \frac{e^{-\delta_h}}{4\pi r_h}(1 - 2m_h'). \tag{30}$$

For the conventional Reissner-Nordström black hole, since $\delta_h \equiv 0$ and $r_h \neq 0$, the temperature approaches zero in the extreme limit where $2m_h' = 1$ is satisfied. In general, since δ_h takes a positive value, r_h must approach zero in the extreme limit for T to remain a finite nonzero value. As we mentioned above, massive dilaton black holes become extreme at the nonzero horizon radius. Thus, the temperature approaches zero in the extreme limit as shown in Fig. 4. So if we consider the evaporation process of the black hole, the small amount of the dilaton mass prevents the black hole from evaporating completely. Unfortunately, since we do not have an analytic solution, we cannot prove it. But as we mention in the following section, our results suggest that these properties are fairly general for general potentials.

B. With $V_2 = m_d^2 S^2 (S-1)^2 e^{S-1}/4$

Here we treat the potential of the rather unusual shape considered in Ref. [10]. But this also approaches $m_d^2\phi^2$ near the asymptotic vacuum as is expected theoretically. So it would be appropriate to investigate the difference and the similarity from $V_1 = m_d^2\phi^2$. We first show the field distributions of the black holes in Fig. 5 [(a) r-ϕ, (b) r-δ, (c) r-m]. We choose $m_d = e/2Q_e$ and e/Q_e for the horizon radius $r_h = 1.1\sqrt{G}$. We show the solution with V_2, V_1 and the approximate solution $\phi = -Q_e^2/m_d^2 r^4$ by solid lines, dashed lines, and dotted lines, respectively. In Fig. 5(a), we can find that the deviation from the $\phi = -Q_e^2/m_d^2 r^4$ near the event horizon for the solution with V_2 is larger than that with V_1, since V_2 has a sharper shape than V_1 for the fixed dilaton mass m_d, which works the role of the large dilaton mass

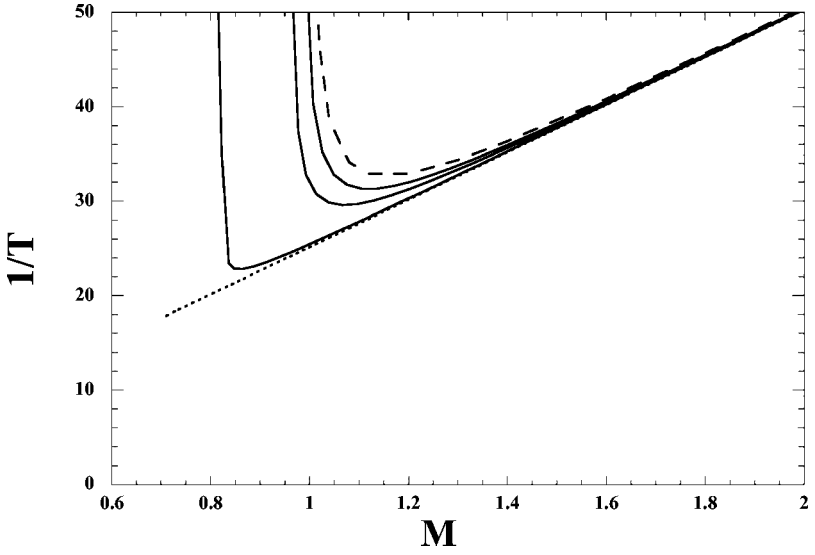

FIG. 4. The relation between the gravitational mass M and the inverse Hawking temperature $1/T$ for the same solutions as in Fig. 3.

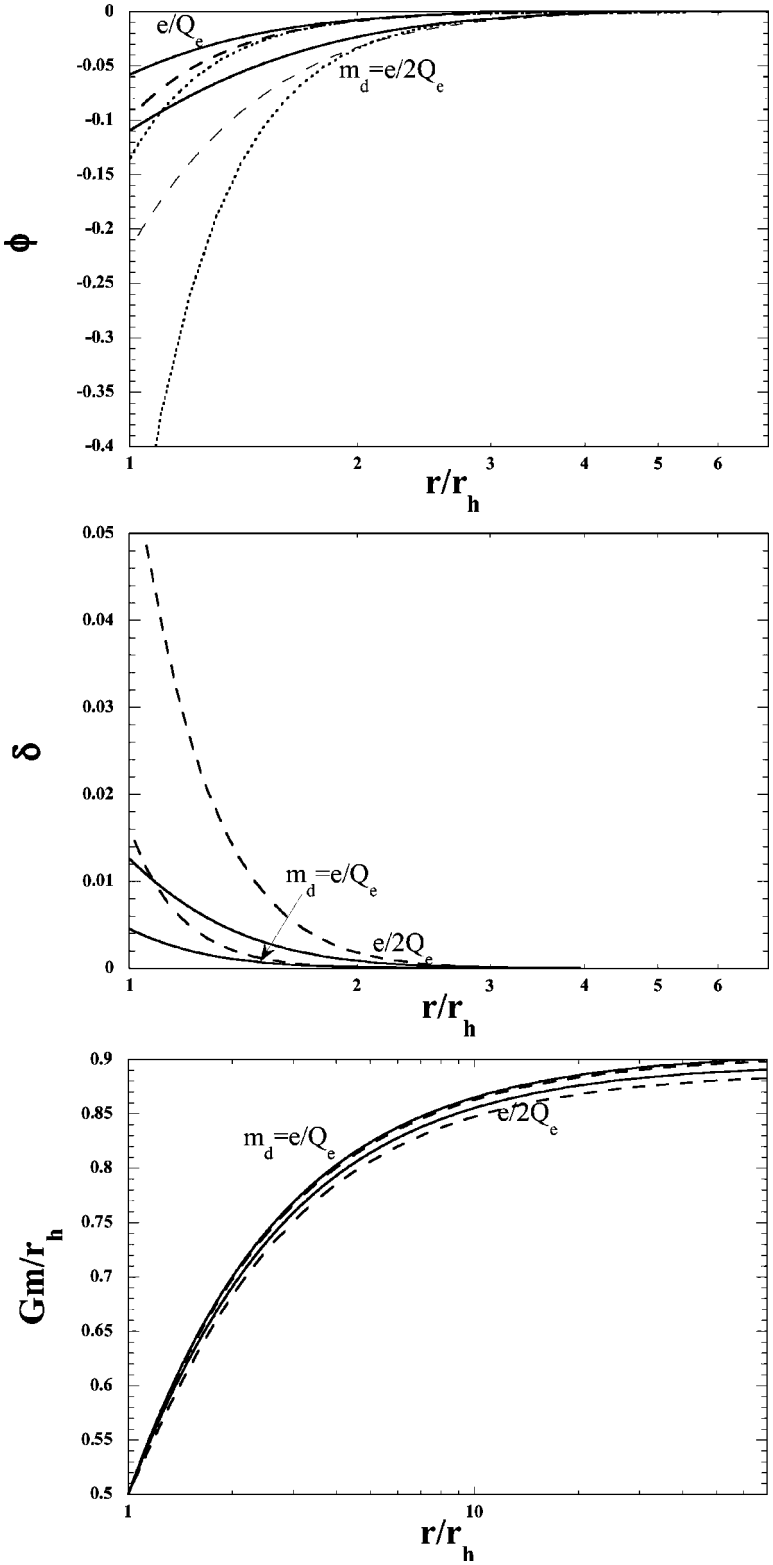

FIG. 5. Field distributions of a massive dilaton black hole with potential V_2 [(a) r-ϕ, (b) r-δ, (c) r-m] with horizon radius $r_h=1.1\sqrt{G}$ and the dilaton mass $m_d=e/2Q_e$ and e/Q_e by solid lines. For comparison, we also show a massive dilaton black hole with V_1 and the approximate solution $\phi=-Q_e^2/m_d^2r^4$ by dashed lines and dotted lines, respectively.

near the horizon effectively, as we see in Fig. 6. Thus, even if the potential approaches $m_d^2\phi^2$ for the vicinity of $\phi=0$, the shapes of the potential become important since ϕ takes a nonzero value near the horizon. This can also be seen in Figs. 5(b) and 5(c). The lapse function δ for V_2 has a smaller value than that for V_1, which implies that the solution for V_2 approaches the RN solution compared with that for V_1. The mass function m also suggests it since the RN black hole has larger gravitational mass compared with that of the GM-GHS solution.

We are also interested in these affects when we consider solutions of a different horizon radius. If we consider the fact that the solutions approach the RN solutions for large m_d while they approach the GM-GHS solutions for small m_d,

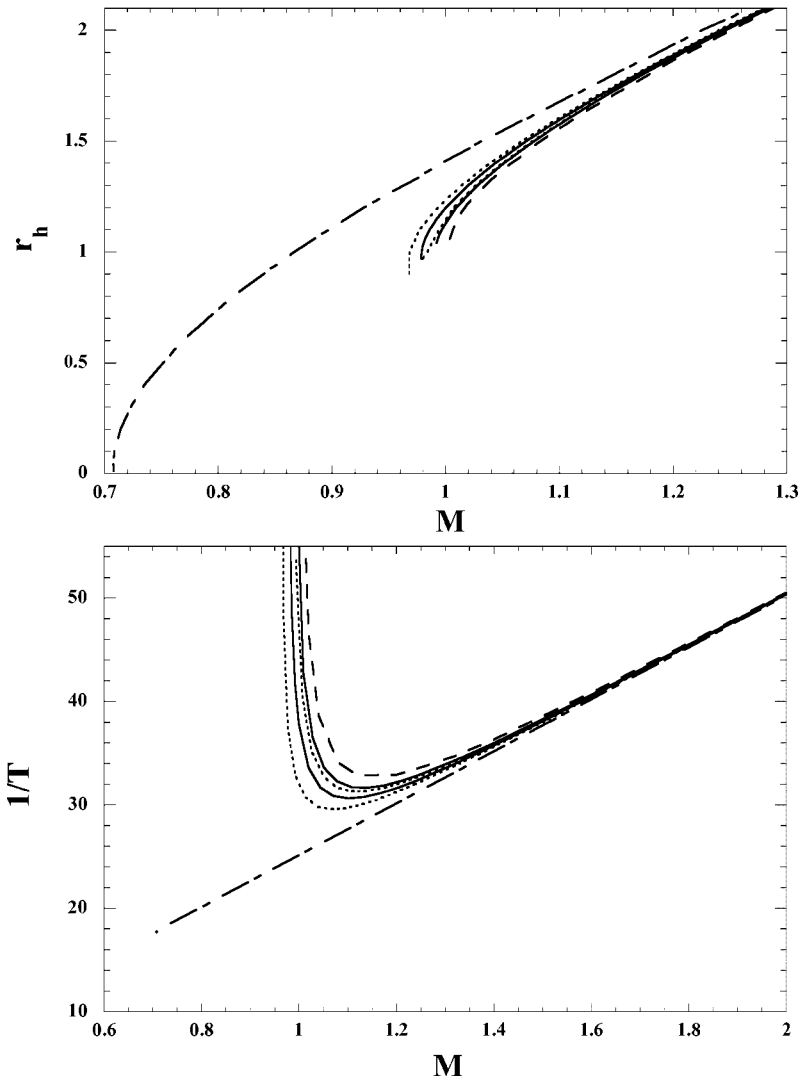

FIG. 6. (a) The horizon radius r_h and (b) the inverse temperature $1/T$ in terms of the gravitational mass M for $m_d=e/2Q_e$ and e/Q_e. We show the solutions with V_2, those with V_1, the GM-GHS solution and the RN solution by solid lines, by dotted lines, by a dashed line, and by a dot-dashed line, respectively.

the answer is simple. The solutions with V_2 approach the RN solution compared with those with V_1 for the same dilaton mass m_d because of the sharpness of the potential. We show the relation between the gravitational mass M and the horizon radius r_h, and the inverse temperature in Figs. 6(a) and 6(b), respectively. We show solutions with V_2 for the dilaton mass $m_d=e/2Q_e$, e/Q_e by solid lines and those with V_1 for the corresponding dilaton mass by dotted lines, respectively. We also show the RN and the GM-GHS solutions by a dashed line and a dot-dashed line, respectively. In Fig. 6(a) we find that if we compare the solution with V_2 to that with V_1 for the same dilaton mass m_d, the deviation of both solutions becomes large near the extreme solution since the dilaton affects the solutions in the region comparable to its Compton wavelength $\sim 1/m_d$. This tendency is also reflected in Fig. 6(b). One of the most important things is that, since the black hole becomes extreme at the finite horizon radius, the temperature inevitably approaches zero in the extreme limit. This does not depend on the potential we choose. At present, since we solved this only numerically, we do not have its proof for general potentials. But we expect it, apart from those with ''pathological'' potential (e.g., that with negative mass or a case that has no regularity near the asymptotic vacuum).

V. CONCLUSION AND DISCUSSION

We have investigated the static spherically symmetric solutions in the Einstein-Maxwell-dilaton system with dilaton potential. We considered the electrically charged solution for the dilaton coupling $\gamma=1$ with the potential $V_1=m_d^2\phi^2$ and $V_2=m_d^2S^2(S-1)^2e^{S-1}/4$ where $S:=e^{-2\phi}$, which is proposed based on gluino condensation. As in previous papers, we have obtained the result that the inner horizon appears for small black holes while the solution has only one horizon for large black holes. The most striking feature we have obtained numerically is that the extreme solution appears for the finite horizon radius when the dilaton has the mass term. As a result, the temperature approaches zero for the extreme limit while it approaches a finite nonzero value for the GM-GHS solution with the dilaton coupling $\gamma=1$. Thus, if we consider the evaporation process of black holes, the small amount of the dilaton mass may change the final fate of the black hole. These properties are quite important, calling for further investigation.

As future research we can consider the following problems. (i) Can we prove the above property for the general potentials? To consider it, it would be necessary to restrict the shapes of potentials, e.g., convex shape. (ii) How about the other dilaton coupling or the magnetically charged solution? These have a direct relation to the present system. In particular, since the GM-GHS solution for $\gamma>1$ has a diverging temperature for the zero horizon limit, the critical dilaton mass parameter $m_{d,crit}(\gamma)$ may exist in which the dilaton black hole approaches the finite nonzero temperature in the extreme limit.

By the way, it may be important to extend the system to such as the Einstein-Yang-Mills-dilaton (EYMD) system with the dilaton potential. Although the EYMD system has been considered before [14–16], that with the potential term has not. Since this system has many qualitative differences from the Einstein-Maxwell-dilaton system, it is worth investigating. For example, there is a particlelike solution in the EYMD system while there is none in the Einstein-Maxwell-dilaton system. This feature may be changed by considering the dilaton potential. This is now under investigation [17].

ACKNOWLEDGMENTS

Special thanks to Hiroshi Watabe and Takashi Torii for useful discussions. T.T is thankful for financial support from the JSPS. This work was supported by a JSPS Grant-in-Aid (No. 106613) and by the Waseda University Grant for Special Research Projects.

[1] R. Ruffini and J. A. Wheeler, Phys. Today **24** (No. 1), 30 (1971).
[2] G. W. Gibbons and K. Maeda, Nucl. Phys. **B298**, 741 (1988); D. Garfinkle, G. T. Horowitz, and A. Strominger, Phys. Rev. D **43**, 3140 (1991).
[3] For a review of no hair conjecture, see [4].
[4] P. Bizon, Acta Phys. Pol. B **25**, 877 (1994).
[5] For the notation, see our action (1).
[6] J. Koga and K. Maeda, Phys. Rev. D **52**, 7066 (1995); T. Tamaki and K. Maeda, *ibid.* **62**, 107503 (2000).
[7] T. Tamaki, K. Maeda, and T. Torii, Phys. Rev. D **57**, 4870 (1998); **60**, 104049 (1999).
[8] C. Will, *Theory and Experiment in Gravitational Physics* (Cambridge Univ. Press, Cambridge, 1981).
[9] R. Gregory and J. A. Harvey, Phys. Rev. D **47**, 2411 (1993); J. H. Horne and G. T. Horowitz, Nucl. Phys. **B399**, 169 (1993).
[10] M. Dine, R. Rohm, N. Seiberg, and E. Witten, Phys. Lett. **156B**, 55 (1985).
[11] W. H. Press, S. A. Teukolsky, W. T. Vetterling, and B. P. Flannery, *Numerical Recipes in FORTRAN* (Cambridge Univ. Press, Cambridge, 1986).
[12] M. Demianski, Found. Phys. **16**, 187 (1986); H. d'Oliveira, Class. Quantum Grav. **11**, 1469 (1994).
[13] T. Tamaki and T. Torii, Phys. Rev. D **62**, 061501 (2000); **64**, 024027 (2001).
[14] G. Lavrelashvili and D. Maison, Nucl. Phys. **B410**, 407 (1993); E. E. Donets and D. V. Gal'sov, Phys. Lett. B **302**, 411 (1993); T. Torii and K. Maeda, Phys. Rev. D **48**, 1643 (1993); C. M. O'Neill, *ibid.* **50**, 865 (1994).
[15] B. Kleihaus, J. Kunz, and A. Sood, Phys. Lett. B **354**, 240 (1995); Phys. Rev. D **54**, 5070 (1996); Phys. Lett. B **374**, 289 (1996); **418**, 284 (1998).
[16] T. Tamaki, K. Maeda, and M. Inada, Phys. Rev. D **63**, 087504 (2001).
[17] T. Tamaki (unpublished).